Thermoelectric Transport in a Three-Channel Charge Kondo Circuit

T. K. T. Nguyen[1,*] and M. N. Kiselev[2]
[1]Institute of Physics, Vietnam Academy of Science and Technology, 10 Dao Tan, Hanoi, Vietnam
[2]The Abdus Salam International Centre for Theoretical Physics, Strada Costiera 11, I-34151, Trieste, Italy

(Received 24 November 2019; accepted 16 June 2020; published 8 July 2020)

We theoretically investigate the thermoelectric transport through a circuit implementation of the three-channel charge Kondo model quantum simulator [Z. Iftikhar *et al.*, Science **360**, 1315 (2018)]. The universal temperature scaling law of the Seebeck coefficient is computed perturbatively approaching the non-Fermi liquid strong coupling fixed point using the Abelian bosonization technique. The predicted $T^{1/3}\log T$ scaling behavior of the thermoelectric power sheds light on the properties of Z_3 emerging parafermions and gives access to exploring prefractionalized zero modes in the quantum transport experiments. We discuss a generalization of approach for investigating a multichannel Kondo problem with emergent $Z_N \to Z_M$ crossovers between "weak" non-Fermi liquid regimes corresponding to different low-temperature fixed points.

DOI: 10.1103/PhysRevLett.125.026801

Quantum thermoelectricity is one of the most rapidly developing directions of quantum technology [1,2]. Modern progress in fabrication of nanodevices operating at ultralow (milli-Kelvin range) temperatures opens access to a broad variety of the charge, spin, and heat transport phenomena governed entirely by the quantum effects [3,4]. In particular, quantization effects in behavior of quantum simulators (see. e.g., [5–12]) at the regimes affected by quantum criticality are challenging for both experimental and theoretical communities.

Among a large variety of available quantum devices, quantum dots (QDs) play an important and significant role. On the one hand, the QD devices [3,4] are highly controllable and fine-tunable setups operating at the regimes adjustable by external electric and magnetic fields at both weak and strong out of equilibrium conditions. On the other hand, the QD devices, as the quantum impurity simulators, provide an important playground for understanding the influence of strong electron-electron interactions, interference effects, and resonance scattering on the quantum transport.

One of the cornerstone effects showing both the resonance scattering and strong interactions as two sides of the same coin is the Kondo effect [13,14]. While a conventional Kondo phenomenon is attributed to a spin degree of freedom of the quantum impurity [15–17], the unconventional charge Kondo effect is dealing with an isospin implementation of the charge quantization [18–23]. The Kondo model [14–16] is one of the known realizations of the "minimal models" archetypal for description of both Fermi liquid (FL) and non-Fermi liquid (NFL) regimes associated with the collective many-body phenomena.

The FL paradigm is one of the most important achievements of twentieth-century condensed matter physics [24]. It provides a tool to account for the effects of interaction in the equilibrium and out-of-equilibrium correlation functions [25]. While FLs are well defined objects characterized by some universal properties of corresponding quantum field theory encoded in scaling behavior of the correlation functions [25] or, equivalently, certain constraints in the phenomenological description, NFLs represent rather *"terra incognita"* unless some strong fingerprints of the quantum behavior inconsistent with the FL paradigm directly follow from known classes of the models. Fortunately, the multichannel Kondo (MCK) model gives access to collective behavior completely different from the FL theory predictions [26–28]. The beauty and "simplicity" of the Kondo model makes it attractive for both experimental implementation of the strongly correlated physics and theoretical benchmarking of the many-body approaches beyond conventional mean-field or perturbation theory techniques. The price one has to pay for using a minimal model is in immense complications in experimental fabrication of the MCK devices [29] and necessity to use advanced and cumbersome theoretical tools for the description of the strong coupling regimes [30–32].

Recently, the breakthrough experiments [11,12] convincingly demonstrated the paramount importance of MCK physics for the quantum charge transport through nanodevices. The few-channel Kondo physics is shown to be extended beyond the existing realization of a two-channel Kondo (2CK) effect [29,33] to a three-channel Kondo (3CK) phenomenon. While the NFL regime of 2CK [34–36] is explained by an emergent Z_2 symmetry attributed to Majorana fermions [30,37], the 3CK physics is known to be associated with Z_3 parafermion states [38–43].

In this Letter, we address a fundamental question regarding how the NFL physics of the 3CK model

influences the quantum thermoelectric transport through the quantum simulators reported in [11,12]. In particular, we theoretically investigate a scaling behavior of thermoelectric coefficients and analyze crossovers between the NFL regimes associated with different low temperature strong coupling fixed points of 3CK. The temperature scaling of thermopower is closely related to corresponding scaling of the fundamental quantum thermodynamic quantities (see [44]) providing (as opposed to electric conductance measurements [11,12]) an access to fractionally quantized entropy [44].

Model.—In a nanodevice (see Fig. 1) designed to be used for thermoelectric measurements [45–48], the drain consists of a large metallic QD electrically connected to two-dimensional electron gas (2DEG) electrodes through three quantum point contacts (QPCs) as proposed in Refs. [11,12]. The 2DEG is in the integer quantum Hall (IQH) regime at the filling factor $\nu = 2$. The QPCs are fine tuned to satisfy the condition that only the outer spin polarized chiral edge current is partially transmitted across the QPCs. The drain is at the reference temperature T. The source is separated from the QD by a tunnel barrier with low transparency $|t| \ll 1$ as described by a tunnel Hamiltonian $H_{\rm tun} = \sum_k (t c_k^\dagger d + \text{H.c.})$ with c and d denoting the electrons in the left lead and in the dot. The temperature of the source can be controlled by the "floating island" technique [5]. A micron-sized metal island [5] is electrically connected by several channels at opposite voltages (to have a zero dc voltage) in the left electrode upstream to the tunnel contact to the Kondo island [49]. Electrons in the floating island are heated up with Joule heat. The resulting temperature is measured by noise-based thermometry [5,49–51]. The temperature difference ΔT across the tunnel barrier is assumed to be small compared to the reference temperature T to guarantee the linear response regime for the device at the weak link [52]. The central metallic island (QD) is in a regime of weak (mesoscopic) Coulomb blockade [21,53] characterized by the charging energy E_C. The gate voltage V_g is used to tune charge degeneracy $N(V_g)$ to the regimes of Coulomb peaks (N is half-integer) and Coulomb valleys (N is integer). The Kondo physics is observed through the measurements of the QPCs differential conductances G_α at zero bias voltages $V_\alpha \to 0$ through the measurement of I_α/V_α [12] (see Fig. 1). The MCK regime is fine tuned by setting transmission coefficients across QPCs to be equal. Applying a thermovoltage $\Delta V_{\rm th}$ to implement a zero-current condition for the electric current between the source (orange lead) and drain (QD and three blue leads) allows us to access the thermoelectric coefficient G_T through the measurements of $I_\alpha/\Delta T$ and Seebeck coefficient, also known as thermopower (TP), $S = G_T/G|_{I=0} = -\Delta V_{\rm th}/\Delta T$ [45].

The mapping of the IQH setup to a MCK problem is explained in detail in Ref. [54]. We assign the isospin $\uparrow$ to the electrons in each QPC and the isospin $\downarrow$ to the electrons in the QD. The charge isospin flips when the electrons move in and out of the QD. Backscattering transfers "moving in" the QD electrons to "moving out" from the QD electrons and vice versa. The number of QPCs is equivalent to the number of orbital channels in the conventional $S = 1/2$ Kondo problem.

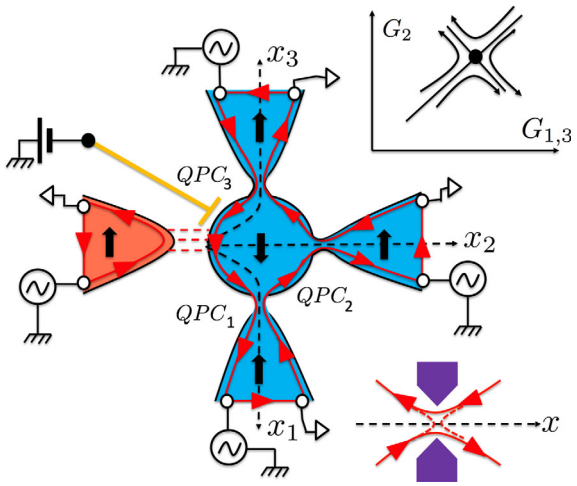

FIG. 1. Schematic of three channel charge Kondo (3CK) setup. A central metallic island, also known as quantum dot (QD), is connected to four electrodes formed by two dimensional electron gas. The state in QD is characterized by the isospin $\sigma = \downarrow$. The states in the electrodes are characterized by the isospin $\sigma = \uparrow$. The left (orange) electrode is heated to the temperature $T + \Delta T$ and connected to the rest of the setup through a tunnel contact (red dashed lines). The reference temperature of the QD and three blue electrodes is T. The yellow plunger gate is used to control a mesoscopic Coulomb blockade in the QD. The setup is fine tuned by an external magnetic field to the integer quantum Hall regime $\nu = 2$. The current propagates along spin-polarized edge channels (red solid lines with arrows). Only one relevant (outer) chiral edge channel is shown. The transparencies of the quantum point contacts QPC_1-QPC_3 (narrow blue constrictions) are controlled by the surface split gates (magenta boxes in insert). Black dashed lines depict three independent x axes with origins located in the middle of constrictions (QD boundary). Zoomed in edge state at one of the QPCs and weak backscattering (red dotted lines) are shown in the lower inset. The identical thermovoltages are applied across the tunnel contacts to nullify the net electric current through the device. Upper inset schematically shows a renormalization group flow for 3CK. The unstable strong coupling fixed point at $G_1 = G_2 = G_3 \approx 0.69 e^2/h$ corresponds to the 3CK non-Fermi-liquid regime.

It is convenient to describe the interacting electrons in the QD and QPCs in the bosonized representation [19–23,55]. We start with the Euclidean action $S = S_0 + S_C + S'$ describing the QD and three QPCs. The action S_0 [32] stands for the free part representing three copies of free one-dimensional electrons in QPC_α

$$S_0 = \frac{v_F}{2\pi} \sum_{\alpha=1}^{3} \int_0^\beta dt \int_{-\infty}^{\infty} dx \left[\frac{[\partial_t \phi_\alpha(x,t)]^2}{v_F^2} + [\partial_x \phi_\alpha(x,t)]^2 \right],$$

Here, $\phi_\alpha(x,t)$ denotes bosonic field describing the transport through QPC$_\alpha$ (see, also, [54]) and v_F is a Fermi velocity [56], $\beta = 1/T$ (we adopt the units $\hbar = c = k_B = 1$).

The effects of the weak mesoscopic Coulomb blockade in the QD are described by the Hamiltonian $H_C = E_C[\hat{n} - N(V_g)]^2$. In the spirit of Andreev-Matveev theory [55], the operator $\hat{n}$ in the Hamiltonian H_C accounts for the electrons entering the dot through the left weak tunnel barrier and three QPCs ($\hat{n} = \hat{n}_L + \hat{n}_{\mathrm{QPC}}$). The number of electrons entering the QD from the QPCs is related to the bosonic fields ϕ_α as $\hat{n}_{\mathrm{QPC}} \to \sum_{\alpha=1}^{3} \phi_\alpha(0,t)/\pi$ [55,57], while the operator $\hat{n}_L$ counting the number of electrons tunneling from the left electrode can be replaced by the function $n_\tau(t) = \theta(t)\theta(\tau - t)$ [55]. Here, $\theta(t)$ is the unit step function (Heaviside function). The Coulomb blockade action S_C in bosonized representation [19–23,55] is given by

$$S_C(\tau) = \int_0^\beta dt E_C \left[n_\tau(t) + \frac{1}{\pi} \sum_{\alpha=1}^{3} \phi_\alpha(0,t) - N(V_g) \right]^2.$$

Finally, the action S'

$$S' = -\frac{D}{\pi} \sum_{\alpha=1}^{3} |r_\alpha| \int_0^\beta dt \cos[2\phi_\alpha(0,t)],$$

characterizes the backscattering at QPCs with r_α as the reflection amplitude for the QPCα, and D is the bandwidth (ultraviolet cutoff). We consider the symmetric situation, where $|r_1| = |r_2| = |r_3| \equiv |r| \ll 1$.

Three normal modes.—We introduce three linear combinations of the fields ϕ_α to represent charge, pseudospin, and flavor modes (see, e.g., [58])

$$\begin{aligned}
\phi_c(x,t) &= \frac{1}{\sqrt{3}}[\phi_1(x,t) + \phi_2(x,t) + \phi_3(x,t)], \\
\phi_s(x,t) &= \frac{1}{\sqrt{2}}[\phi_1(x,t) - \phi_3(x,t)], \\
\phi_f(x,t) &= \frac{1}{\sqrt{6}}[\phi_1(x,t) - 2\phi_2(x,t) + \phi_3(x,t)], \qquad (1)
\end{aligned}$$

and the same for the dual boson fields $(1/\pi)\partial_x\theta_\alpha = \Pi_\alpha = -(1/v_F)\partial_t\phi_\alpha$ satisfying equal-time commutation relations: $[\phi_\alpha(x), \Pi_{\alpha'}(x')] = i\delta(x - x')\delta_{\alpha\alpha'}$ [30–32]. Here, α, α' denote charge, pseudospin $S = 1$, and flavor. The pseudospin and flavor modes are related to two diagonal Gell-Mann matrices of the SU(3) group [4,59]. The parametrization (1) explicitly breaks the symmetry between QPCs, while this symmetry is preserved in the model. Therefore, we need to use two additional parametrizations [60] corresponding to the cyclic permutations of the indices $1 \to 2 \to 3$ (renumeration of the QPCs) and apply a symmetrization procedure at the point $|r_\alpha| = |r|$. For brevity, we omit index labeling the representation [60] in the notations.

The action in the charge, pseudospin, and flavor modes (for illustration, we use (1) $\vec{\phi}_{csf} \equiv \vec{\phi}^{\mu}$ [60]) is

$$S_0 = \frac{v_F}{2\pi} \int_0^\beta dt \int_{-\infty}^{\infty} dx \sum_{\alpha=c,s,f} \left[\frac{[\partial_t \phi_\alpha(x,t)]^2}{v_F^2} + [\partial_x \phi_\alpha(x,t)]^2 \right], \qquad (2)$$

$$S_C(\tau) = \int_0^\beta dt E_C \left[n_\tau(t) + \frac{\sqrt{3}}{\pi} \phi_c(0,t) - N(V_g) \right]^2, \qquad (3)$$

$$\begin{aligned}
S' = -\frac{D}{\pi}|r| \int_0^\beta dt \Bigg\{ &\cos\left[\frac{2}{\sqrt{3}} \phi_c(0,t) - \frac{2\sqrt{2}}{\sqrt{3}} \phi_f(0,t) \right] \\
&+ 2\cos\left[\frac{2}{\sqrt{3}} \phi_c(0,t) + \frac{\sqrt{2}}{\sqrt{3}} \phi_f(0,t) \right] \cos[\sqrt{2}\phi_s(0,t)] \Bigg\}. \qquad (4)
\end{aligned}$$

Action S_0 is particle-hole (PH) symmetric. PH transformation in the action S_C corresponds to change from N to $-N$ (electrons are replaced by holes). As a result, the transport coefficients G and G_T transform under PH transformation as follows: $G(N) = G(-N)$ and $G_T(-N) = -G_T(N)$. Besides, the thermoelectric transport requires breaking of the particle-hole symmetry described by the backscattering action S'.

Furthermore, due to the Coulomb blockade effect, all transport coefficients are periodic in $N(V_g)$ and the action is invariant with respect to the shift $N \to N + 1$. To show it, we notice that the electron travels from or to the QD, to or from one of the QPCs. In the setup (see Fig. 1), there are three possible ways to do it: (i) electron enters QD from the QPC1: $\phi_1 \to \phi_1 + \pi$, $\phi_2 \to \phi_2$, $\phi_3 \to \phi_3$. As a result $\phi_c \to \phi_c + \pi/\sqrt{3}$, $\phi_s \to \phi_s + \pi/\sqrt{2}$, $\phi_f \to \phi_f + \pi/\sqrt{6}$; (ii) electron enters QD from the QPC2: $\phi_1 \to \phi_1$, $\phi_2 \to \phi_2 + \pi$, $\phi_3 \to \phi_3$, then $\phi_c \to \phi_c + \pi/\sqrt{3}$, $\phi_s \to \phi_s$, $\phi_f \to \phi_f - 2\pi/\sqrt{6}$; and (iii) electron enters QD from the QPC3: $\phi_1 \to \phi_1$, $\phi_2 \to \phi_2$, $\phi_3 \to \phi_3 + \pi$, then $\phi_c \to \phi_c + \pi/\sqrt{3}$, $\phi_s \to \phi_s - \pi/\sqrt{2}$, $\phi_f \to \phi_f + \pi/\sqrt{6}$. These discrete transformations keep the backscattering action S' invariant and increase the charge of the QD by one. We rely upon these transformations (as well as corresponding transformations in basis $\vec{\phi}^{\lambda}$ and $\vec{\phi}^{\rho}$ [60]) in the perturbative calculations (see details in [61]).

Perturbative calculations.—The transport coefficients G and G_T are expressed in terms of the correlation function $K(\tau)$ [55]

$$\begin{aligned}
K(\tau) &= Z(\tau)/Z(0), \\
Z(\tau) &= \int \exp[-S_0 - S_C(\tau) - S'] \prod_\alpha \mathcal{D}\phi_\alpha(x,t). \qquad (5)
\end{aligned}$$

This correlation function is characterized by the following symmetries associated with PH and shift transformation: $K(\beta-\tau,N)=K(\tau,1-N)$ and $K(\beta-\tau,N)=K(\tau,-N)$.

The electric conductance G [20] is given by

$$G=\frac{G_L\pi T}{2}\int_{-\infty}^{\infty}\frac{1}{\cosh^2(\pi T t)}K\left(\frac{1}{2T}+it\right)dt. \quad (6)$$

Here, $G_L \ll e^2/h$ denotes the tunnel conductance of the left barrier calculated ignoring influence of the dot. The thermoelectric coefficient G_T takes the form [55]

$$G_T=-\frac{i\pi^2}{2}\frac{G_L T}{e}\int_{-\infty}^{\infty}\frac{\sinh(\pi T t)}{\cosh^3(\pi T t)}K\left(\frac{1}{2T}+it\right)dt. \quad (7)$$

The correlator $K(\tau)$ acquires a simple form in the absence of the backscattering. The action S_0+S_C is Gaussian and the functional integrals are explicitly evaluated resulting in [62] (see details of calculations in [61])

$$K(\tau)|_{r=0}=K^{(0)}(\tau)=\left[\frac{\pi^2 T}{3\gamma E_C}\frac{1}{|\sin(\pi T\tau)|}\right]^{2/3}. \quad (8)$$

Here, $\gamma=e^{\mathbf{C}}\approx 1.78$, $\mathbf{C}\approx 0.577$. The backscattering $r\neq 0$ explicitly breaks the PH symmetry. However, the mechanism of the PH symmetry breaking is different for the FL ($M=1$) and MCK-NFL, ($M\geq 2$) states. Namely, for the FL case, there exists only one gapped mode associated with the charge. Therefore, the PH symmetry breaking occurs already in the first order of the perturbation theory [55]. If, however, there are $M-1$ gapless modes describing spin and flavors for the MCK-NFL, the first order perturbative correction vanishes, and PH symmetry breaking occurs in the second order. The nonvanishing contribution to the G_T and S is associated with the fluctuations of $M-1$ gapless modes. We process with the perturbative calculations at the second order $K^{(2)}(\tau)=K_C(\tau)(\langle S'^2\rangle_\tau-\langle S'^2\rangle_0)/2$. The validity of the perturbation theory at $|r|^2\ll 1$ for 2CK [55] is justified by the condition for the temperature regime $T^*\ll T\ll E_C$ where $T^*=|r|^2E_C$ [55]. We refer to this regime as the weak NFL regime.

Scaling of transport coefficients.—The main contribution to the electric conductance does not depend on $|r|$. Its temperature scaling is fully determined by the form of $K^{(0)}(\tau)$ given by Eq. (8) (see [63,68])

$$G\sim G_L[T/E_C]^{2/3}. \quad (9)$$

We compute the perturbative contribution to the thermoelectric coefficient G_T proportional to $|r|^2$ [61] with log-accuracy using three parametrizations of the charge, pseudospin, and flavor modes and symmetrize over three QPC index permutations (renumerations) [60]. Finally, each QPC contributes equally to G_T

$$G_T\sim\frac{G_L}{e}|r|^2\sin(2\pi N)[1+a\cos(2\pi N)]\left[\frac{T}{E_C}\right]\ln\left[\frac{E_C}{T}\right]. \quad (10)$$

with $a\sim 1$ [61]. Substituting Eqs. (10) and asymptotic equation for G Eq. (9) into the definition of the TP $S=G_T/G$, we obtain [69]

$$S\sim\frac{1}{e}|r|^2\sin(2\pi N)[1+a\cos(2\pi N)]\left[\frac{T}{E_C}\right]^{1/3}\ln\left[\frac{E_C}{T}\right]. \quad (11)$$

The perturbative 3CK results for G_T (10) and TP (11) do not diverge at the limit $T\to 0$ in contrast to 2CK predictions [55]. Besides, the temperature scaling of TP $S^{3\mathrm{CK}}\propto T^{1/3}\log T$ is consistent with the corresponding nonperturbative scaling of the TP maximums $S^{2\mathrm{CK}}_{\max}\propto T^{1/2}\log T$ for 2CK. In both cases, S vanishes when $T\to 0$. Therefore, we expect that the scaling (11) will survive at the limit $T\to 0$ and acquire only marginal modifications in the argument of log [55]. Equations (10)–(11) represent the central result of this Letter.

Channel symmetry breaking.—We comment on possible ways to crossover 3CK → 2CK and 3CK → 1CK in the charge Kondo circuits. These crossovers have been experimentally reported in [11,12] and numerically reproduced in [70–72] by using the numerical renormalization group (NRG) technique. The simplest way to describe continuous crossover of 3CK → 2CK is to imbalance, e.g., the reflection amplitudes in QPC1 and QPC3 [73]. Having $a_{13}\equiv||r_1|-|r_3||$ as a relevant perturbation to the symmetric state characterized by $s_{13}\equiv(|r_1|+|r_3|)/2\approx|r|$ provides a condition for a crossover $a_{13}\sim s_{13}$ similar to the theory of channel symmetry breaking of 2CK → 1CK discussed in [52]. In addition, the condition $a_{13}s_{13}\ll|r_2|^2\approx|r|^2$ is required. However, one needs to go beyond the perturbation theory for the quantitative description of the crossover. The mechanism of 3CK → 1CK is more delicate. First, the experiment [12] shows the nonmonotonic behavior of conductance evolution confirmed by nonmonotonic NRG flow in numerical calculations [70–72]. Second, the crossover regime has to be fine tuned by the condition $|a_{13}s_{13}-|r_2|^2|\ll|r_2|^2$. Discussion of these regimes goes beyond the scope of this Letter and will be published elsewhere [74].

Discussion and open questions.—Describing the quantum thermoelectricity in the NFL regime of the MCK model at the strong coupling limit $T\ll T^*$ is one of the main open questions. In particular, it is important to understand if there exists a re(para)fermionization procedure for the Z_3 fixed point similar to the Emery-Kivelson (EK) approach [37] developed for $U(1)\to Z_2$ symmetry reduction [75]. The EK refermionization being a cornerstone for the understanding of the emergence of the NFL

state of 2CK is known to allow straightforward reformulation of the strong coupling Hamiltonian in terms of Z_2 Majorana (para)fermions. However, even if such a procedure does exist for the Z_3 low temperature fixed point [76], the strong coupling Hamiltonian will not be quadratic anymore in terms of the Z_3 parafermions [77]. Therefore, the nonperturbative treatment of the 3CK problem at its strong coupling will require some additional assumptions or approximations. Yet another challenging question is related to the generalization of the approach developed in this Letter for the description of the $M > 3$ MCK effect at the strong coupling. We expect that even and odd M-channel models behave significantly differently: while the ground state of the even-$M = 2k$ channel models can be represented in terms of the Majorana fermions [78], Z_{2k+1} parafermions are needed for the description of the odd-$M = 2k + 1$-channel Kondo physics. Besides, switching between Z_{2k+1} and Z_{2k} low temperature fixed points opens an interesting possibility for investigation of the crossovers between states with different parafermion fractionalized zero modes. The same goal can be achieved by using the quantum simulators containing a tunnel contact between two different NFL states [54].

Conclusions.—In this Letter, we theoretically address a fundamental question of the prefractionalized zero mode's influence on the quantum thermoelectricity of nanodevices. Using an asymptotically exact analytic approach based on Abelian bosonization, we predict the fractional $T^{1/3} \log T$ low-temperature scaling behavior of the Seebeck coefficient. While this scaling is obtained perturbatively at the weak NFL regime, we also present convincing arguments on the validity of the results at the strong coupling limit. The fractional scaling of the quantum thermoelectric transport coefficients is closely related to behavior of quantum thermodynamic observables [79]. We propose to use an experimental technique [12] providing the circuit implementation of quantum simulators of the MCK model for investigation of the parafermion contribution to the quantum thermoelectricity controlled by switching the quantum regimes between different low temperature fixed points.

We are grateful to Leonid Glazman, Yuval Gefen, Joel Moore, Yuval Oreg, and Alexander Nersesyan for illuminating discussions. We are especially grateful to Frederic Pierre for the detailed explanation of the experiments [11,12], suggestions [50] for the experimental realization of the thermoelectric measurements with quantum simulators [49], and discussion of the dynamical Coulomb blockade effects [63,64]. We acknowledge the warm hospitality of the Center for Theoretical Physics of Complex Systems (PCS) of the Institute for Basic Science (IBS) and the International Centre of Physics (ICP) of the Institute of Physics (IOP—VAST). T. K. T. N. acknowledges support through the ICTP Associate Program, ICTP Asian Network on Condensed Matter and Complex Systems, and International Centre of Physics under Grant No. ICP.2020.03. This research in Hanoi is funded by the Vietnam National Foundation for Science and Technology Development (NAFOSTED) under Grant No. 103.01-2020.05. The work of M. K. was performed in part at Aspen Center for Physics, which is supported by National Science Foundation Grant No. PHY-1607611 and was partially supported by a grant from the Simons Foundation.

Note added.—Recently, a preprint on thermoelectrics of 2CK [80] considering a closely related problem was posted in the cond-mat archive.

*Corresponding author.
nkthanh@iop.vast.ac.vn

[1] G. Benenti, G. Casati, K. Saito, and R. S. Whitney, Phys. Rep. **694**, 1 (2017).
[2] V. Zlatic and R. Monnier, *Modern Theory of Thermoelectricity* (Oxford University Press, Oxford, 2014).
[3] Y. M. Blanter and Y. V. Nazarov, *Quantum Transport: Introduction to Nanoscience* (Cambridge University Press, Cambridge, England, 2009).
[4] K. Kikoin, M. N. Kiselev, and Y. Avishai, *Dynamical Symmetry for Nanostructures. Implicit Symmetry in Single-Electron Transport Through Real and Artificial Molecules* (Springer, New York, 2012).
[5] S. Jezouin, F. D. Parmentier, A. Anthore, U. Gennser, A. Cavanna, Y. Jin, and F. Pierre, Science **342**, 601 (2013).
[6] S. Jezouin, Z. Iftikhar, A. Anthore, F. D. Parmentier, U. Gennser, A. Cavanna, A. Ouerghi, I. P. Levkivskyi, E. Idrisov, E. V. Sukhorukov, L. I. Glazman, and F. Pierre, Nature (London) **536**, 58 (2016).
[7] E. Sivre, A. Anthore, F. D. Parmentier, A. Cavanna, U. Gennser, A. Ouerghi, Y. Jin, and F. Pierre, Nat. Phys. **14**, 145 (2018).
[8] M. Banerjee, M. Heiblum, V. Umansky, D. E. Feldman, Y. Oreg, and A. Stern, Nature (London) **559**, 205 (2018).
[9] M. Banerjee, M. Heiblum, A. Rosenblatt, Y. Oreg, D. E. Feldman, A. Stern, and V. Umansky, Nature (London) **545**, 75 (2017).
[10] H. Inoue, A. Grivnin, N. Ofek, I. Neder, M. Heiblum, V. Umansky, and D. Mahalu, Phys. Rev. Lett. **112**, 166801 (2014).
[11] Z. Iftikhar, S. Jezouin, A. Anthore, U. Gennser, F. D. Parmentier, A. Cavanna, and F. Pierre, Nature (London) **526**, 233 (2015).
[12] Z. Iftikhar, A. Anthore, A. K. Mitchell, F. D. Parmentier, U. Gennser, A. Ouerghi, A. Cavanna, C. Mora, P. Simon, and F. Pierre, Science **360**, 1315 (2018).
[13] J. Kondo, Prog. Theor. Phys. **32**, 37 (1964).
[14] A. Hewson, *The Kondo Problem to Heavy Fermions* (Cambridge University Press, Cambridge, England, 1993).
[15] A. M. Tsvelik and P. B. Wiegmann, Adv. Phys. **32**, 453 (1983).
[16] N. Andrei, K. Furuya, and J. H. Lowenstein, Rev. Mod. Phys. **55**, 331 (1983).
[17] L. Kouwenhoven and L. I. Glazman, Phys. World **14**, 33 (2001).

[18] K. Flensberg, Phys. Rev. B **48**, 11156 (1993).
[19] K. A. Matveev, Phys. Rev. B **51**, 1743 (1995).
[20] A. Furusaki and K. A. Matveev, Phys. Rev. B **52**, 16676 (1995).
[21] I. L. Aleiner and L. I. Glazman, Phys. Rev. B **57**, 9608 (1998).
[22] K. Le Hur, Phys. Rev. B **64**, 161302(R) (2001).
[23] K. Le Hur and G. Seelig, Phys. Rev. B **65**, 165338 (2002).
[24] L. D. Landau, ZhETF **30**, 1058 (1957) [Sov. Phys. JETP **3**, 920 (1957)], http://www.jetp.ac.ru/cgi-bin/e/index/e/3/6/p920?a=list; ZhETF**32**, 59 (1957) [Sov. Phys. JETP**5**, 101 (1957)], http://www.jetp.ac.ru/cgi-bin/e/index/e/5/1/p101?a=list.
[25] P. Coleman, *Introduction to Many-Body Physics* (Cambridge University Press, Cambridge, England, 2015).
[26] P. Nozières and A. Blandin, J. Phys. France **41**, 193 (1980).
[27] D. Cox and A. Zawadowski, Adv. Phys. **47**, 599 (1998).
[28] I. Affleck and A. W. W. Ludwig, Phys. Rev. B **48**, 7297 (1993).
[29] R. M. Potok, I. G. Rau, H. Shtrikman, Y. Oreg, and D. Goldhaber-Gordon, Nature (London) **446**, 167 (2007).
[30] A. O. Gogolin, A. A. Nersesyan, and A. M. Tsvelik, *Bosonization and Strongly Correlated Systems* (Cambridge University Press, Cambridge, England, 1999), https://books.google.it/books?id=g2CBQgAACAAJ&source=gbs_book_other_versions.
[31] T. Giamarchi, *Quantum Physics in One Dimension* (Oxford University Press, Oxford, 2004).
[32] D. Sènèchal, An introduction to bosonization, edited by D. Sènèchal, A. M. Tremblay, and C. Bourbonnais, in *Theoretical Methods for Strongly Correlated Electrons*, CRM Series in Mathematical Physics (Springer, New York, 2004).
[33] Y. Oreg and D. Goldhaber-Gordon, Phys. Rev. Lett. **90**, 136602 (2003).
[34] N. Andrei and C. Destri, Phys. Rev. Lett. **52**, 364 (1984).
[35] M. Fabrizio, A. O. Gogolin, and Ph. Nozières, Phys. Rev. Lett. **74**, 4503 (1995).
[36] M. Fabrizio, A. O. Gogolin, and Ph. Nozières, Phys. Rev. B **51**, 16088 (1995).
[37] V. J. Emery and S. Kivelson, Phys. Rev. B **46**, 10812 (1992).
[38] A. B. Zamolodchikov and V. A. Fateev, ZhETF **89**, 380 (1985) [Sov. Phys. JETP **62**, 215 (1985)], http://www.jetp.ac.ru/cgi-bin/e/index/e/62/2/p215?a=list.
[39] H. Yi and C. L. Kane, Phys. Rev. B **57**, R5579 (1998).
[40] H. Yi, Phys. Rev. B **65**, 195101 (2002).
[41] I. Affleck, M. Oshikawa, and H. Saleur, Nucl. Phys. **B594**, 535 (2001).
[42] C. Nayak, S. H. Simon, A. Stern, M. Freedman, and S. D. Sarma, Rev. Mod. Phys. **80**, 1083 (2008).
[43] J. Alicea and P. Fendley, Annu. Rev. Condens. Matter Phys. **7**, 119 (2016).
[44] Y. Kleeorin, H. Thierschmann, H. Buhmann, A. Georges, L. W. Molenkamp, and Y. Meir, Nat. Commun. **10**, 5801 (2019).
[45] R. Scheibner, H. Buhmann, D. Reuter, M. N. Kiselev, and L. W. Molenkamp, Phys. Rev. Lett. **95**, 176602 (2005).
[46] R. Scheibner, E. G. Novik, T. Borzenko, M. Konig, D. Reuter, A. D. Wieck, H. Buhmann, and L. W. Molenkamp, Phys. Rev. B **75**, 041301(R) (2007).
[47] A. Svilans, M. Josefsson, A. M. Burke, S. Fahlvik, C. Thelander, H. Linke, and M. Leijnse, Phys. Rev. Lett. **121**, 206801 (2018).
[48] B. Dutta, D. Majidi, A. G. Corral, P. A. Erdman, S. Florens, T. A. Costi, H. Courtois, and C. B. Winkelmann, Nano Lett. **19**, 506 (2019).
[49] F. Pierre (private communication).
[50] Alternatively, the heating of the left electrode (Fig. 1) can be achieved by injection of some energy with the voltage biased QPC located upstream of the tunnel contact [49,51]. The electrons relax after some adjustable propagation distance to a "hot" Fermi distribution characterized by the temperature $T + \Delta T$ measured by the noise thermometry [5].
[51] H. le Sueur, C. Altimiras, U. Gennser, A. Cavanna, D. Mailly, and F. Pierre, Phys. Rev. Lett. **105**, 056803 (2010).
[52] T. K. T. Nguyen, M. N. Kiselev, and V. E. Kravtsov, Phys. Rev. B **82**, 113306 (2010).
[53] S. Amasha, I. G. Rau, M. Grobis, R. M. Potok, H. Shtrikman, and D. Goldhaber-Gordon, Phys. Rev. Lett. **107**, 216804 (2011).
[54] T. K. T. Nguyen and M. N. Kiselev, Phys. Rev. B **97**, 085403 (2018).
[55] A. V. Andreev and K. A. Matveev, Phys. Rev. Lett. **86**, 280 (2001); K. A. Matveev and A. V. Andreev, Phys. Rev. B **66**, 045301 (2002).
[56] The integration in S_0 is performed along three independent axes x_1, x_2, x_3 (see Fig. 1). The x-axis label is dummy and, therefore, will be omitted.
[57] The fluctuating charge (in units of e) in the dot area is equal to $\pi^{-1}\int_{-\infty}^{0}\sum_{\alpha=1}^{3}\partial_x\phi_\alpha(x,t)dx \to \pi^{-1}\sum_{\alpha=1}^{3}\phi_\alpha(0,t)$ [21] (only the boundary term is left).
[58] M. Fabrizio and A. O. Gogolin, Phys. Rev. B **50**, 17732(R) (1994).
[59] In general, for M species of the electrons, the normal modes are charge, spin, and $M-2$ flavor modes. Thus, $M-1$ modes describing spin and all flavors are connected to the Cartan (Abelian) subgroup of the corresponding SU(M) group [4].
[60] Two diagonal Gell-Mann matrices of the fundamental representation of the SU(3) group are denoted as $\lambda_3 = \mathrm{diag}[1,-1,0] \equiv -\lambda_s$ and $\lambda_8 = \mathrm{diag}[1,1,-2]/\sqrt{3} \equiv \lambda_f$. These matrices form the λ-Cartan basis. We add the unit matrix to describe the charge mode: $\lambda_0 = \mathrm{diag}[1,1,1] \equiv \sqrt{3/2}\lambda_c$. The transformation from the basis labeling QPC (1–3): $\vec{\phi}_{123}(x,t) = (\phi_1\phi_2\phi_3)^T$ to the basis of charge, pseudospin, and flavor modes c, s, f: $\vec{\phi}^{\lambda}_{csf}(x,t) = (\phi_c\phi_s\phi_f)^T$ is given by $\phi^{\lambda}_{\alpha} = 1/\sqrt{2}\ \mathrm{Tr}[\lambda_\alpha\cdot\vec{\phi}_{123}]$ where $\alpha = c,\ s,\ f$. We define two additional bases of the Gell-Mann matrices through the linear combination of the λ-Cartan basis: $\mu_3 = (\lambda_3+\sqrt{3}\lambda_8)/2 \equiv \mu_s$, $\mu_8 = (\sqrt{3}\lambda_3-\lambda_8)/2 \equiv \mu_f$, $\rho_3 = (\lambda_3-\sqrt{3}\lambda_8)/2 \equiv \rho_s$, $\rho_8 = (\sqrt{3}\lambda_3+\lambda_8)/2 \equiv -\rho_f$. Corresponding transformation to the csf basis is given by $\phi^{\mu}_{\alpha} = 1/\sqrt{2}\ \mathrm{Tr}[\mu_\alpha\cdot\vec{\phi}_{123}]$ and $\phi^{\rho}_{\alpha} = 1/\sqrt{2}\ \mathrm{Tr}[\rho_\alpha\cdot\vec{\phi}_{123}]$ with $\mu_c = \rho_c = \lambda_c$. The Jacobian for all transformations $|J| = 1$.
[61] See Supplemental Material at http://link.aps.org/supplemental/10.1103/PhysRevLett.125.026801 for perturbative calculations of the thermoelectric coefficient G_T.

[62] Importantly, for general MCK, we define the charge mode $\phi_c(x,t) = [\phi_1(x,t) + \cdots + \phi_M(x,t)]/\sqrt{M}$. Only the charge mode enters the charging energy action. Therefore, the correlator $K_C(\tau) = \{\pi^2 T/[M\gamma E_C|\sin(\pi T\tau)|]\}^{2/M}$.

[63] The temperature dependence of the electric conductance $G \propto (T/E_C)^{2/3}$ given by (9) exactly corresponds to the dynamical Coulomb blockade scaling [49]. This dependence was experimentally observed recently [64]. The scaling (9) is consistent with the orthogonality catastrophe [65–67] explanation given in Ref. [20].

[64] A. Anthore, Z. Iftikhar, E. Boulat, F. D. Parmentier, A. Cavanna, A. Ouerghi, U. Gennser, and F. Pierre, Phys. Rev. X **8**, 031075 (2018).

[65] P. W. Anderson, Phys. Rev. Lett. **18**, 1049 (1967).

[66] P. Nozières and C. T. de Dominicis, Phys. Rev. **178**, 1097 (1969).

[67] G. D. Mahan, *Many Particle Physics* (Plenum, New York, 1991).

[68] This scaling is also valid in the strong coupling regime $T \ll T^*$ since Eq. (9) corresponds to the zeroth order term of the perturbative expansion in $|r|^2$.

[69] The temperature scaling of G_T for $M \geq 2$ channel Kondo model is, in general, described by $G_T \propto T^{1-2/M+2/M} \log T \sim T \log T$ behavior and, thus, in log approximation, does not depend on M (up to M-dependent prefactor). The $\log T$ behavior of G_T is associated with the fluctuations of $M-1$ gapless modes (spin and flavors) and is generic for all $M \geq 2$ channel charge Kondo models characterized by the NFL behavior. The gate voltage oscillating dependence is described by $\sin[2\pi N(V_g)]$ factor accounting for the charge quantization. The TP scaling is given by $S^{\mathrm{MCK}} \propto T^{1-2/M} \log T$. The TP of all MCK models vanishes at low temperature being, however, strongly enhanced by $\log T$ factor compared to $S^{1\mathrm{CK}} \propto T$ FL scaling.

[70] E. Sela, A. K. Mitchell, and L. Fritz, Phys. Rev. Lett. **106**, 147202 (2011).

[71] A. K. Mitchell, L. A. Landau, L. Fritz, and E. Sela, Phys. Rev. Lett. **116**, 157202 (2016).

[72] L. A. Landau, E. Cornfeld, and E. Sela, Phys. Rev. Lett. **120**, 186801 (2018).

[73] When the symmetry between QPCs is explicitly broken, we use the Cartan basis compatible to the model with broken symmetry.

[74] T. K. K. Nguyen and M. N. Kiselev (to be published).

[75] T. K. T. Nguyen and M. N. Kiselev, Phys. Rev. B **92**, 045125 (2015).

[76] P. L. S. Lopes, I. Affleck, and E. Sela, Phys. Rev. B **101**, 085141 (2020); Y. Komijani, Phys. Rev. B **101**, 235131 (2020).

[77] K. Snizhko, F. Buccheri, R. Egger, and Y. Gefen, Phys. Rev. B **97**, 235139 (2018).

[78] P. Lecheminant, A. O. Gogolin, and A. A. Nersesyan, Nucl. Phys. **B639**, 502 (2002).

[79] E. Sela, Y. Oreg, S. Plugge, N. Hartman, S. Lüscher, and J. Folk, Phys. Rev. Lett. **123**, 147702 (2019).

[80] G. A. R. van Dalum, A. K. Mitchell, and L. Fritz, Phys. Rev. B **102**, 041111 (2020).